

## A new method for *in line* electrokinetic characterization of cakes

Yannick Lanteri<sup>1</sup>, Wael Ballout<sup>2</sup>, Patrick Fievet<sup>\*2</sup>, Sébastien Déon<sup>2</sup>,  
Anthony Szymczyk<sup>3</sup> and Patrick Sauvade<sup>4</sup>

<sup>1</sup> Institut Européen des Membranes, 34095 Montpellier cedex 5, France

<sup>2</sup> Institut UTINAM, Université de Franche-Comté, 25030 Besançon cedex, France

<sup>3</sup> Université de Rennes 1, Institut des Sciences Chimiques de Rennes, 35042 France

<sup>4</sup> Degremont Technologie - AQUASOURCE, 31029 Toulouse, France

(Received June 12, 2012, Revised February 05, 2013, Accepted April 13, 2013)

**Abstract.** The present study is devoted to the validation of a new method for in line electrokinetic characterisation of deposits on membrane surfaces. This method is based upon simultaneous measurements of transversal streaming potential and permeates flux at constant pressure before and during the deposit formation. Dead-end filtration experiments were conducted with negative flat membranes forming a narrow slit channel, negative hollow fiber membranes and mono-dispersed suspensions of (negatively charged) polystyrene latex and (positively charged) melamine particles at various concentrations. It was observed that the overall streaming potential coefficient increased in absolute value with the deposited latex quantity, whereas it decreased and changed of sign during the filtration of melamine suspensions. By considering a resistance-in-series model, the streaming potential coefficient of the single deposit ( $SP_d$ ) was deduced from the electrokinetic and hydraulic measurements. The independence of  $SP_d$  with respect to growth kinetics validates the measurement method and the reliability of the proposed procedure for calculating  $SP_d$ . It was found that  $SP_d$  levelled off much more quickly when filtration was performed through the slit channel. This different behaviour could result from a non-uniform distribution of the deposit thickness along the membrane given that the position of measuring electrodes is different between the two cells.

**Keywords:** electrokinetics; streaming potential; particles; latex; melamine; cakes; fouling; dead-end filtration; hollow fibers

### 1. Introduction

Micro- and ultrafiltration membrane processes are widely used to filter complex fluids (such as wastewaters or surface waters) containing micro-organisms, colloidal and/or dissolved species. However, membrane fouling, especially fouling by the deposition of suspended materials during filtration is always posing a main obstacle for wider application of these processes. When the foulants are much larger than that the membrane pores themselves, they tend to form a cake layer on the external membrane surface, causing a permeate flux reduction. The magnitude of the flux decline depends on both structure (thickness, porosity...) and surface (surface charge density)

---

\*Corresponding author, Professor, E-mail: [patrick.fievet@univ-fcomte.fr](mailto:patrick.fievet@univ-fcomte.fr)

properties of fouling layers, the later having also an impact on their growth and morphological properties and thus, on their transport properties (permeate flux and solute rejection). Different methods are available to determine the surface electric properties of porous media. Among them, streaming potential measurement has become, thanks to its experimental simplicity, the most widely used method for characterizing the electrokinetic charge of the clean and fouled membranes. Streaming potential arises when there is a relative motion between the fluid containing charged species and charged surface caused by a hydrostatic pressure gradient (Hunter 1981). This parameter is believed to be correlated with the interactions between the membrane surface and various charged foulants. Studies dedicated to the characterization of fouled membranes by streaming potential are scarce and can be divided into two categories: ex-situ studies for which the streaming potential of the virgin membrane and fouled membrane are measured before and after fouling, and in-situ studies for which the streaming potential is monitored during fouling. The latter are obviously more favorable because they provide dynamic information on electrokinetic behaviour during membrane fouling.

Le Bolay and Ricard (1995) studied time evolution of transversal streaming potential coefficient (streaming potential-to-applied pressure ratio) during filtration of an albumin suspension on acrylate MF membrane. For a pH around 5.2, they observed two different variations of the streaming potential coefficient time evolution, which were linked to the flux decline trends and to a possible change of fouling mechanisms. However, no relation between time behaviour of streaming potential coefficient and fouling layer properties was proposed. More recently, Chun *et al.* (2002, 2004) and Sung *et al.* (2003) investigated time evolution of transversal streaming potential during dead-end and cross-flow filtration of colloids or proteins. In the case of membranes and latex colloids, which have the same charge sign, these authors found that absolute values of the streaming potential coefficient tend to decrease with the progress of filtration in dead-end mode whereas an opposite trend was observed in a cross-flow mode. The decreasing behaviour was attributed to the reduction of the electrokinetic flow through the pores due to the development of the cake layer. According to the authors, the cross-flow characteristic would allow the particles to stay mainly in a suspended state above the outer surface of the membrane, forming a concentration polarization layer, rather than being deposited onto the surface (Chun *et al.* 2002, 2004). As a result, the streaming potential coefficient would increase during the filtration because of the increasing effect of the concentration gradient. Irrespective of the filtration mode, it was also shown that both the cake layer thickness and particle concentration inside the cake increased with the increasing particle concentration of the suspension. In another study, the authors studied the behaviour of the streaming potential during the filtration of bovine serum albumin (BSA) solution under different surface charge conditions in crossflow filtration (Sung *et al.* 2003). The time evolution of the streaming potential coefficient for opposite charge conditions (positively charged membrane and negatively charged latex) showed a reversal of charge sign resulting from BSA deposition onto the outer surface of the membrane. For the same charge sign conditions, the streaming potential coefficient was considerably increased with the filtration progress. As previously, this behaviour was explained by the development of a concentration polarization layer during the cross-flow filtration.

It should be noted that in all these works, the streaming potential was measured by applying discrete pressure steps during the filtration at a given transmembrane pressure, with the system allowed to equilibrate at each pressure step. However, no information is given about the impact of transmembrane pressure steps on fouling layer properties. It should be noted that in most practical situations, the filtration of fluids containing particles or proteins leads to compressible deposits

(Chloe *et al.* 1986, Gourgues *et al.* 1992, Murase *et al.* 1995, Hamachi and Mietton-Peuchot 1986, Mendret *et al.* 2009). In such conditions, the application of overpressures might disturb the deposit formation (and thus, its structure properties) and influence the measurements themselves. Indeed, the compactness of the deposit might increase the conductivity of electrolyte inside deposit (due to a decrease in pore size) and thus, decrease the measured potential in the streaming potential experiments (Szymczyk *et al.* 2002). As a result, the streaming potential coefficient would be dependent on the pressure difference.

Very recently, Teychene *et al.* (2011) developed a method that consists in measuring the transmembrane streaming potential at constant pressure during the cake layer build-up. Their method was applied to the electrokinetic characterisation of a MF polysulfone membrane during fouling by latex particles. Their results show that for a given mass of particles deposited on the membrane, the variation rate of the electric potential during fouling is directly linked to the transmembrane pressure and varies as the fouling rate. On the other hand, at constant pressure, the amplitude of the electric potential variation increases with deposited particle mass. Their method has the advantage not to disturb the build-up of the cake layer due to the no-variation of the pressure. However, the streaming potential occurring across the “membrane + deposit” structure is an overall signal, which does not reflect the electrokinetic properties of the sole active layer (i.e., the layer of interest).

In this context, a new method for the characterisation of surface electrical properties of sole particle deposits during dead-end filtration was developed. The characterization is based upon simultaneous transversal streaming potential and permeates flux measurements at constant pressure before and during the deposit formation. In order to validate the method, fouling experiments were conducted with calibrated rigid spherical particles of the same charge sign and opposite charge to the membrane through flat membranes forming a narrow channel and hollow fiber membranes.

## 2. Theory

### 2.1 Streaming potential

Let us consider a charged porous medium brought into contact with an electrolyte solution. A charge excess takes place in the electrical double layer that forms inside pores at the solid-liquid interface. When a pressure gradient is applied through the porous medium, the charges in the mobile diffuse layer are carried toward the low-pressure side. This constitutes a streaming current. The accumulation of charge at one end sets up an electric field which causes a conduction current in the opposite direction of the streaming current. When the conduction current equals the streaming current, a steady state is achieved (Hunter 1981). The resulting electric potential difference that can be measured between the pore ends is the streaming potential ( $\Delta\varphi_s$ ). However, it is useful to express the streaming potential as the electrical potential difference per unit pressure ( $SP = \Delta\varphi_s/\Delta P$ ) because this quantity is more informative than the single value of electrical potential difference (which depends on the pressure difference on either side of the porous medium).

It is important to keep in mind that the streaming potential occurring across a “membrane + deposit” structure is an overall signal, which is necessarily influenced by the membrane itself because of the non-negligible pressure drop occurring through it. In addition, the contributions of the membrane and deposit to the overall streaming potential vary with the progress of filtration because of pressure drop variations occurring through both the membrane and cake layer during

the filtration. It is then important to find a method allowing the determination of the streaming potential coefficient of the sole cake layer during its growth. The method proposed is based on simultaneous transversal streaming potential and permeate flux measurements at constant pressure on the sole membrane and the “membrane + deposit” structure.

By considering a resistance-in-series model and applying Darcy’s law and conservation law for volume flux across the two-layer structure, the streaming potential coefficient of the deposit ( $SP_d$ ) can be expressed as follows

$$SP_d = \frac{SP_{m+d} - SP_m(Lp_{m+d} / Lp_m)}{1 - (Lp_{m+d} / Lp_m)} \quad (1)$$

where the symbol  $Lp$  denotes the hydraulic permeability, the subscript  $m$  referring to the membrane and  $m + d$  to the “membrane + deposit” structure.

It should be emphasized that the validity of Eq. (1) implies that the streaming potential coefficient of deposit is independent of pressure drop across it. During the cake formation, the fraction of the constant applied pressure acting on both the membrane and the deposit is changing. For porous layers formed by large particles, the streaming potential coefficient is expected to be independent of the deposit pore size due to the presence of large pores (the surface conductance contribution is negligible in conditions of sufficiently large pore radius in respect with the electrical double layer thickness). In this case, a compaction of deposit should not influence its streaming potential coefficient. On the contrary, the streaming potential coefficient of the deposits formed by small particles is expected to depend on pore size (the surface conductance becomes non-negligible as compared with the conductivity of bulk electrolyte). In these conditions, Eq. (1) is always valid provided that the deposit does not compact otherwise the streaming potential coefficient becomes dependent on the pressure drop across the layer and Eq. (1) is not valid anymore. In order to ensure that no significant compaction occurs, the streaming potential of the deposit must be measured at various external pressures. The working external pressure must then be chosen in the pressure range where the streaming potential varies linearly with the pressure, i.e., where the streaming potential coefficient of the deposit is independent of the pressure (Szymczyk *et al.* 2002).

## 2.2 Deposit permeability

From a resistance-in-series model and applying Darcy’s law and conservation law for volume flux across the two-layer structure, the permeability of deposit ( $SP_d$ ) on membrane surface can be written as follows

$$Lp_d = \frac{Lp_m Lp_{m+d}}{Lp_m - Lp_{m+d}} \quad (2)$$

For dead-end filtration under constant pressure (and in the absence of particle back-transport), the permeability  $Lp$  decreases with time and the mass of deposited particles,  $m_d$ , at the membrane surface can be expressed as

$$m_d = V_c C \quad (3)$$

where  $V_c$  is the cumulated volume of the permeate and  $C$  the particle concentration of the suspension.

According to filtration theory, the deposit permeability can also be related to its specific resistance  $\alpha$  by (Park *et al.* 2007)

$$Lp_d = \frac{A_m}{\mu C V_c \alpha} \quad (4)$$

where  $A_m$  is the membrane surface area and  $\mu$  the viscosity of solution.

If the deposit is considered as a porous stack of solid spheres, its specific resistance can also be related to particle properties by the Carman-Kozeny equation (Karode 2001, Park *et al.* 2007)

$$Lp_d = \frac{\phi_p^2 \varepsilon^3}{\mu t 180 (1-\varepsilon)^2} \quad (5)$$

with

$$t = \frac{m_d}{A_m (1-\varepsilon) d_p} \quad (6)$$

where  $\phi_p$  denotes the particle diameter,  $\varepsilon$  the deposit porosity,  $t$  the deposit thickness and  $d_p$  the particle density.

Eqs. (5) and (6) show that deposit porosity ( $\varepsilon$ ) can be assessed during filtration from deposit permeability ( $Lp_d$ ) measurements as a function of the mass of deposited particles ( $m_d$ ) provided that others parameters ( $A_m$ ,  $d_p$ ,  $\phi_p$ ) are known.

### 3. Experimental

#### 3.1 Membranes and suspensions

Filtration tests were performed with polystyrene latex and melamine suspensions using flat-sheet polyethersulfone and hollow fiber polysulfone membranes. The properties of particles and membranes are given in Table 1.  $10^{-3}$  M KCl solutions and particle suspensions with concentrations of 150, 450 and 750 mg L<sup>-1</sup> in  $10^{-3}$  M KCl solutions were filtered. All solutions and suspensions were prepared from salt of pure analytical grade (Fisher Scientific) and milli-Q quality water (conductivity < 1  $\mu$ S cm<sup>-1</sup>). Their pH was adjusted at  $5.5 \pm 0.1$ . Given the size of colloids and membrane pores, total rejection of particles is expected during filtration.

#### 3.2 Experimental set-up

The experimental set-up used in this work is depicted in Fig. 1. It is composed of a ZETACAD (CAD Inst., France) zeta-meter (Fig. 1(a)), an in-house-built measuring cell for flat sheet (Figs. 1(b) and (c)) or hollow fiber (Fig. 1(d)) membranes and an electronic balance (Sartorius, Model TE31025) connected to a PC.

The filtration cell for flat sheet membranes is a sandwich-type cell with narrow parallelepiped-shaped channel formed by a couple of identical membranes. The channel is formed by clamping together two identical flat membranes separated by a PTFE spacer of 1 mm in thickness, each membrane being positioned in a PMMA plate. Two Ag/AgCl wire electrodes (named “E” in Figs. 1(b) and (c)) are placed just at the inlet of the channel on both sides of one of the two membranes,

Table 1 Properties of particles and membranes used for filtration experiments and dimensions of confined channels

<b>Particles</b>		
	Polystyrene latex	Melamine
Manufacturer	Granuloshop (France)	
shape	Spherical	
Volume median diameter $\phi_p \pm$ standard deviation (nm)	530 $\pm$ 25	480 $\pm$ 30
Particle density $d_p$ (g cm <sup>-3</sup> )	1.05	1.50
<b>Membranes</b>		
	Polyethersulfone	Polysulfone
Manufacturer	Orelis (France)	Degrémont Technologies-Aquasource (France)
Molecular weight cut-off (kDa)		150
Pure water permeability $L_p$ (L h <sup>-1</sup> m <sup>-2</sup> bar <sup>-1</sup> )	240 $\pm$ 20	600 $\pm$ 50
Mean pore size ( $\mu$ m)	~ 0.1	
<b>Channels</b>		
	Slit	Tubular
Geometry and dimensions	length: 278 mm; width: 2 mm; height: 1 mm	length: 140 mm; internal diameter: 0.8 mm
Filtration surface area (cm <sup>2</sup> )	11	3.5

and linked to a Keithley multimeter (model 2000) to measure the electrical potential difference occurring across the membrane.

The filtration cell for hollow fiber membranes is composed of two PTFE cylinders inside which the ends of a PMMA tube (external diameter: 20 mm) containing one hollow fiber is inserted. The ends of the fiber are potted with epoxy resin over ~30 mm in length. The tube is maintained inside the two cylinders with two screwcaps. One of the two cylinders is equipped with a rod-type Ag/AgCl electrode positioned at 20 mm from the end of the fiber. A second rod-type Ag/AgCl electrode is fixed on the PMMA tube to measure the inner potential of the permeate. As previously, the two electrodes are connected to the Keithley multimeter (model 2000) to measure the transmembrane electrical potential difference. The advantage of this cell lies in the possibility to perform measurements for fibers with different dimensions.

Filtration was conducted in dead-end mode at constant transmembrane pressure close to 1 bar. For this, the cells were connected to the zeta-meter by a piping network that enabled filtration to be operated. The liquid was forced through the cell using the nitrogen gas. The gas pressure was controlled by means of a differential pressure sensor (0-1 bar). The choice of the solution to be filtered (solution in the tank 1 or 2) is controlled by a 3-way valve. Therefore, with this set-up, two solutions can be filtered in-series through a membrane without change of transmembrane pressure. The zeta-meter is driven by a PC by means of software (Testpoint<sup>TM</sup>), which also enables the

pressure, electrical potential, conductivity and temperature to be acquired. Thanks to another data acquisition program (SartoConnect Version 3.5, Sartorius), the permeate mass is also monitored in order to determine the permeate flux time variations.

### 3.3 Measuring procedure

The standard experimental procedure for determining the streaming potential of a membrane consists in measuring the electrical potential difference ( $\Delta\phi_s$ ) resulting from a pressure step ( $\Delta P$ ) applied at one side of the membrane when the steady state is reached. The streaming potential

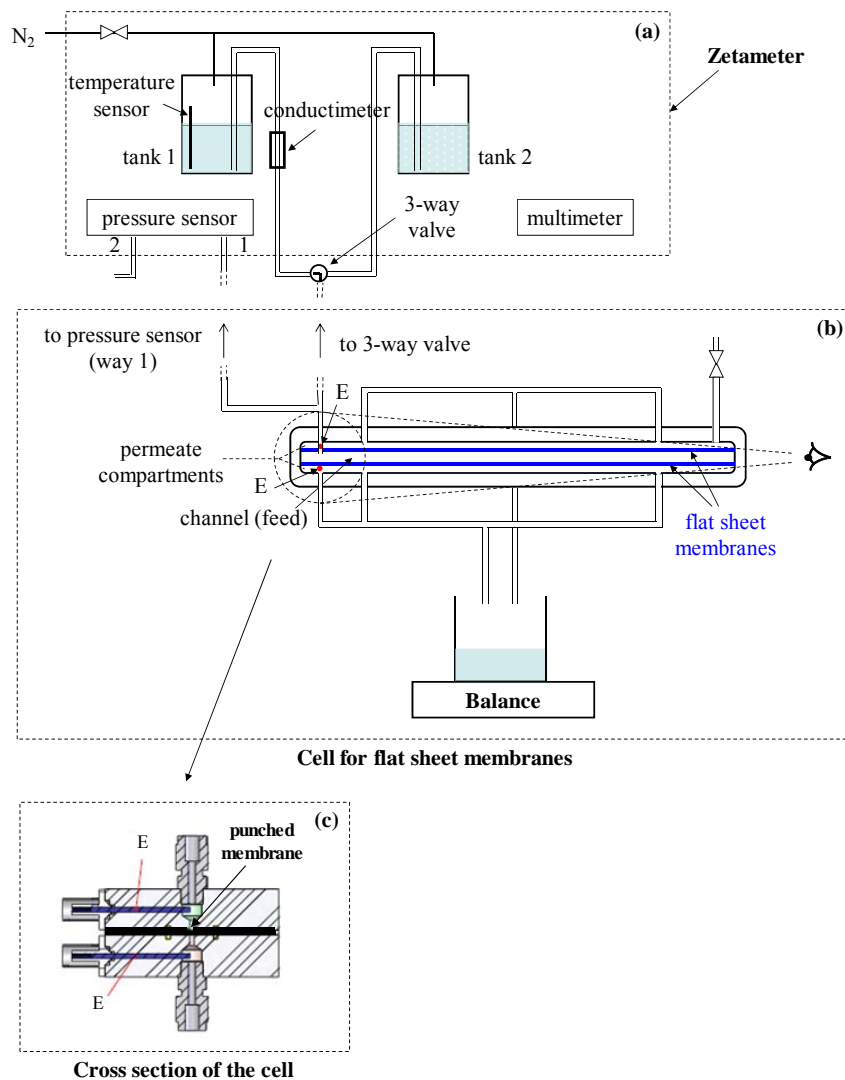


Fig. 1 Schematic representation of the zetameter (a), cell for flat sheet membranes (b) (cross section of the cell (c)) and cell for hollow fiber membranes (d). E: Ag/AgCl electrodes

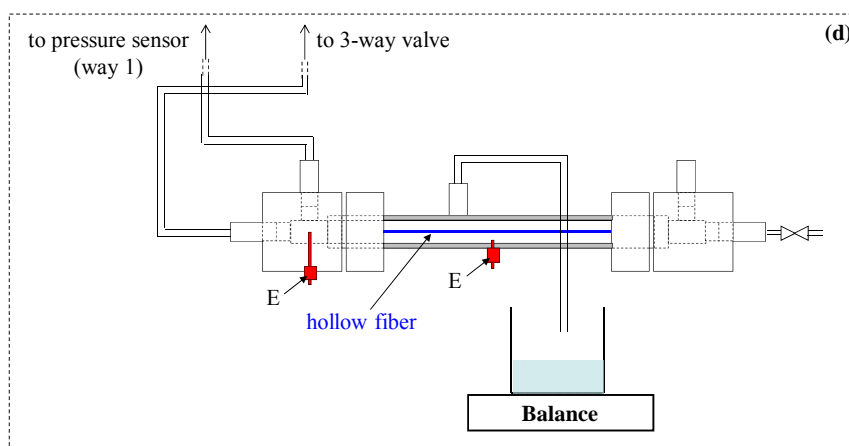


Fig. 1 Continued

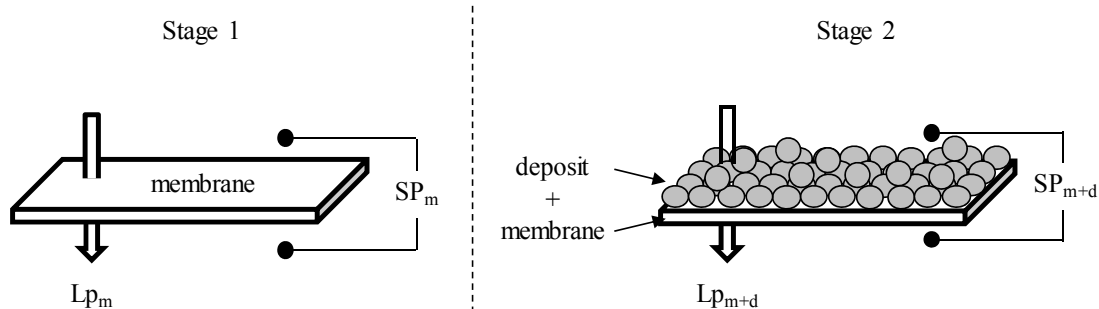


Fig. 2 Schematic representation of the two stages of a filtration experiment and measurements performed during these stages

coefficient is usually determined from a series of  $\Delta\phi_s$  measurements performed at various pressure steps (Nyström *et al.* 1994, 1995). The SP value is then deduced from the slope of the plot of  $\Delta\phi_s$  versus  $\Delta P$ .

In the case of compressible deposits, this procedure is not really favourable since the application of pressure steps during the filtration might affect the deposit structure properties and thus, the measurements themselves. Indeed, the compactness of the deposit (which leads to the decrease of the pore size) might increase the conductivity inside pores and thus, affect the measured potential in the streaming potential experiments (Szymczyk *et al.* 2002). Consequently, streaming potential (and permeate flux) measurements were carried out at constant pressure, according to the following procedure. The KCl solution inside the tank 1 (Fig. 1(a)) was first forced through the membrane(s) by applying pressure difference close to 1 bar (between 940 and 970 mbar), so as to equilibrate the membrane(s) with the measuring solution. During this stage (stage 1), both permeate volume flux and streaming potential were recorded. The filtration of the electrolyte solution was carried out until the flux can be considered as constant (variation of the mean flux less than 2% over a period of 15 min). When the flux was stationary, the streaming

potential also remained constant. The fouling solution (i.e., a latex or melamine suspension) contained in the tank 2 (Fig. 1(a)) was next filtered instead the electrolyte solution under the same pressure by acting on the 3-way valve (stage 2). After the filtration of a given permeate volume (corresponding to some deposited particle mass), the electrolyte solution was filtered again (stage 3). During the stages 1 and 2, the following parameters could be determined (Fig. 2).

- The permeability ( $Lp_m$ ) and streaming potential coefficient ( $SP_m$ ) of the unfouled membrane;
- The overall permeability ( $Lp_{m+d}$ ) and streaming potential coefficient ( $SP_{m+d}$ ) of the “membrane + deposit” structure, during fouling;

For each filtration test, new membrane samples were used. They were first rinsed with milli-Q quality water for 1h under a working pressure of  $\sim 1$  bar before use. Next, the membrane permeability was determined with a  $10^{-3}$  M KCl solution from a series of permeate flux measurements performed at various transmembrane pressures. Finally, the streaming potential coefficient was measured with the same electrolyte applying pressure steps (from 0 to 1 bar) before implementing the stages 1 to 3. At the end of stage 3, the streaming potential of the fouled membrane (membrane + deposit) was also measured at various pressure values by decreasing by steps the transmembrane pressure until to zero.

#### 4. Results

A typical example of the permeability and streaming potential coefficient variation as a function of the deposited particle mass during the filtration of latex or melamine suspensions is shown in Figs. 3a and b for the flat sheet membranes and 3c for the hollow fiber. As can be seen, the filtration of the suspensions leads to a gradual decrease of the permeability and streaming potential coefficient (stage 2). Regarding the overall streaming potential coefficient ( $SP_{m+d}$ ), an opposite behaviour is observed between the two suspensions. It should be noted that both permeability and streaming potential coefficient level off when the filtration of the suspension is stopped and replaced by the one of KCl solution (stage 3). An increase of the absolute value of the streaming potential coefficient with deposited mass is observed with latex suspension. The two membranes being negatively charged ( $SP_m = -5.2$  and  $-6.2$  mV/bar for flat sheet and hollow fiber membranes, respectively), this increase (in absolute value) means that the streaming potential coefficient of the deposit ( $SP_d$ ) is higher (in absolute value) than the one of the membrane. Indeed, in a previous work, it was shown that the overall streaming potential coefficient of a two-layer structure is bounded between the streaming potential coefficients of the two layers when a series association of these layers is considered (Szymczyk *et al.* 1998, 2002). Moreover, it was found that the relative contribution of a layer to the overall electrical signal depends on the hydraulic permeability ratio between both layers. Given that the permeate flux is identical through the membrane and deposit, the hydraulic permeability ratio  $Lp_m/Lp_d$  equals to the reciprocal pressure drop ratio  $\Delta P_d/\Delta P_m$ . Thus, at the beginning of the latex filtration, the overall electrical signal is dominated by the membrane, then, as the deposition proceeds, the contribution of the deposit to the overall streaming potential coefficient increases due to the increase in the pressure drop (that is, the driving force that gives rise to the streaming potential phenomenon) across the deposit and decreases across the membrane. A different behavior is observed with the melamine suspension: the streaming potential coefficient increases and its sign is reversed from negative to positive for some quantity of deposited particles. It can be shown from Eq. (1) that  $SP_{m+d}$  equals zero when  $SP_m Lp_d = -SP_d Lp_m$ .

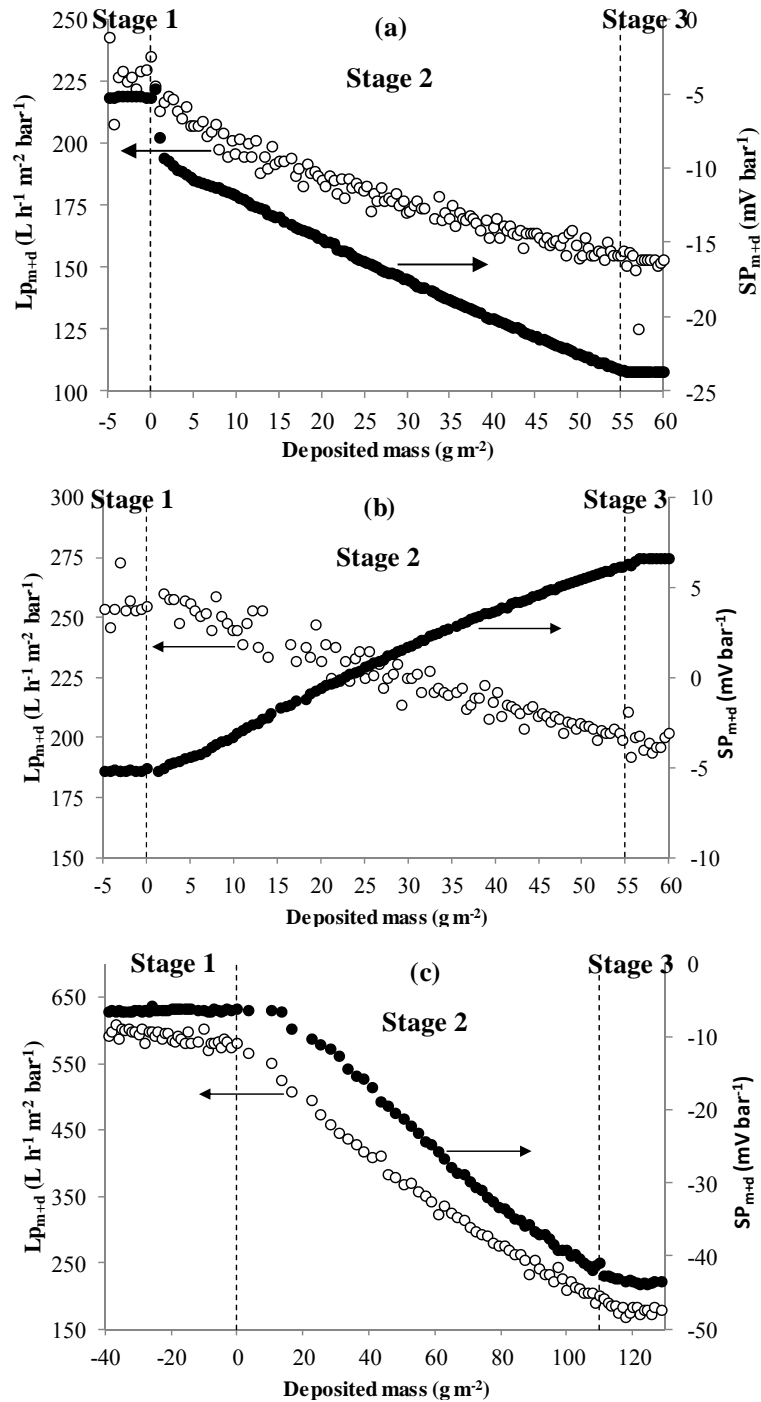


Fig. 3 Permeability ( $Lp_{m+d}$ ) and streaming potential coefficient ( $SP_{m+d}$ ) vs. deposited particle mass during filtration of a (a) latex suspension (450  $mg\ L^{-1}$ ) through a flat membrane at 965  $\pm$  10 mbar, (b) melamine suspension (450  $mg\ L^{-1}$ ) through a flat membrane at 950  $\pm$  8 mbar and (c) latex suspension (750  $mg\ L^{-1}$ ) through a hollow fiber at 955  $\pm$  8 mbar. Stages 1 and 3: filtration of a  $10^{-3}$  M KCl solution

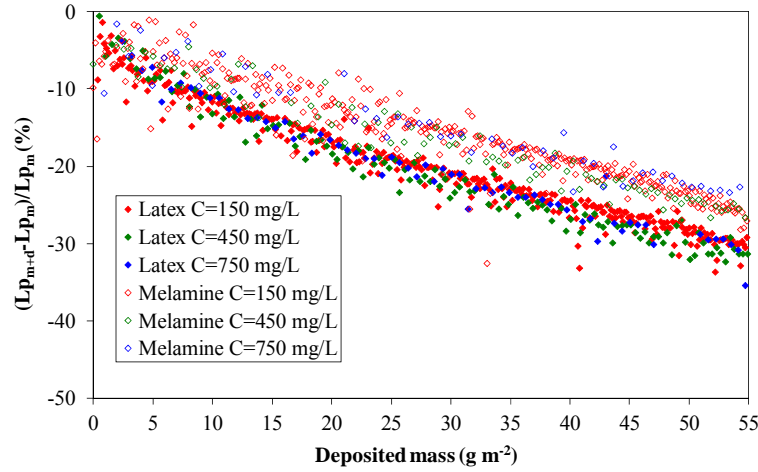


Fig. 4 Relative variation of the permeability ( $(Lp_{m+d} - Lp_m)/Lp_m$ ) vs. deposited particle mass during filtration of latex and melamine suspensions at various particle concentrations (150, 450 and 750 mg L<sup>-1</sup>)

Fig. 4 shows the relative variation of the permeability versus deposited particle mass during the filtration of latex and melamine suspensions for the flat sheet membrane. It appears that the permeability drop is not influenced by particle concentration for the two suspensions. In other words, for a given structure, is not influenced by the deposition kinetics, which is higher for 750 mg L<sup>-1</sup> than for 150 mg L<sup>-1</sup>. It is also seen that the permeability decrease is larger for the latex suspension than for the melamine one. However, no conclusion can be drawn because the latex and melamine particles have neither the same density nor the same size.

Thanks to measurements of  $Lp$  and  $SP$  performed during the stages 1 and 2 of filtration (Fig. 3(a)-(c)), the streaming potential coefficient of the alone deposit ( $SP_d$ ) can be determined from Eq. (1). The variation of  $SP_d$  as a function of deposited particle mass for various latex and melamine concentrations is shown in the case of flat sheet membranes in Fig. 5(a). Firstly, it must be kept in mind that when the cake is not thick enough and consequently, not resistive enough to the flow, as compared to the membrane, it does not contribute significantly to the overall streaming potential. Consequently, the  $SP_d$  values calculated at the beginning of the deposition are not really reliable. As can be seen, beyond some deposited mass,  $SP_d$  tends to the same value (-66 mV bar<sup>-1</sup> and +40 mV bar<sup>-1</sup>) for latex and melamine deposits, respectively), regardless of the particle concentration, i.e., the deposition kinetics. If particles, which are mono-dispersed and rigid, pile up one upon another in an identical way during the filtration, it is then expected that the mean pore size of the cake layer does not vary during its growth and does not depend on growth kinetics. In these conditions, it is quite normal that  $SP_d$  varies neither with the deposit thickness nor with the growth kinetics, since they are the same particles with the same surface charge density that participate in the cake growth. This result confirms the validity of the streaming potential method at constant pressure, as well as reliability of the proposed procedure for assessing the streaming potential coefficient of the sole deposit during its build-up.

As shown in Fig. 5(b), the same asymptotic behavior with a similar  $SP_d$  value (-60 mV bar<sup>-1</sup>) is observed in the case of the hollow fiber. This result is also a proof of the reliability of the proposed procedure since the streaming potential coefficient of the sole deposit is independent of the

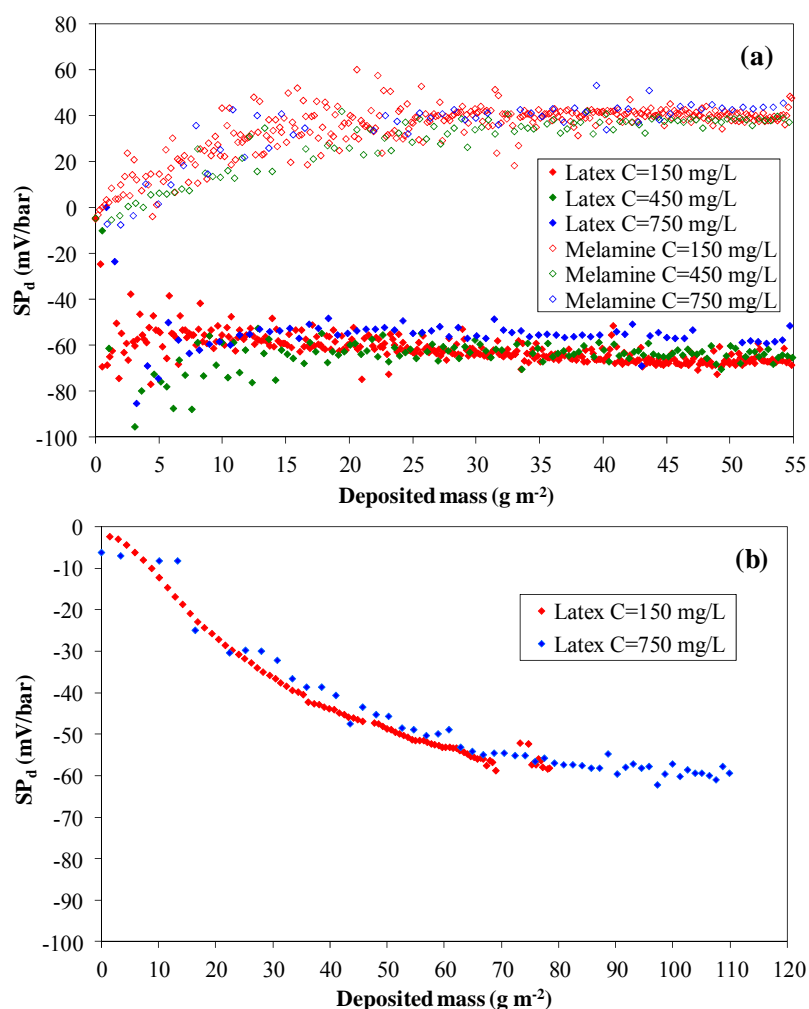


Fig. 5 Streaming potential coefficients of (a) latex and melamine deposits ( $SP_d$ ) vs. deposited particle mass in the case of flat sheet membranes and (b) latex deposits ( $SP_d$ ) vs. deposited particle mass in the case of hollow fiber membranes

substrate on which it builds up. It is also seen that  $SP_d$  is not affected by the particle concentration, i.e., the deposition kinetics, since curves for two different particle concentrations overlap each other. However, it appears that the particle mass to be deposited to reach the asymptotic value is much larger in the case of the hollow fiber ( $\sim 80\ g\ m^{-2}$  opposed to  $\sim 15\ g\ m^{-2}$  for flat membranes). This difference could be the result of a non-uniform distribution of the deposit thickness along the membrane (for both fiber and flat membranes) and the position of measuring electrodes, which is different between the two cells (the two electrodes are positioned at the inlet of the channel for flat membranes whereas one is fixed at the inlet and the other at the middle of the channel for the hollow fiber). Indeed, if the cake is thicker at the inlet of the channel and decreases continuously along the channel, its contribution to the overall streaming potential is expected to be stronger at the inlet and less at the middle of the channel, for a given deposited mass value. Since the  $SP_d$

value can be considered as a local value whereas the deposited mass is a mean value on the whole membrane surface, it means that the deposited mass beyond which  $SP_d$  becomes constant is underestimated for flat membranes (Fig. 5(a)) whereas it is overestimated for the hollow fiber (Fig. 5(b)). It should be mentioned that such longitudinal variations of cake thickness were highlighted by Mendret *et al.* (2010) during ultrafiltration of clay suspension in a confined slit channel using an optical method.

The asymptotic values of  $SP_d$  lead to zeta potentials in the range -12.6 – -11.5 mV for latex

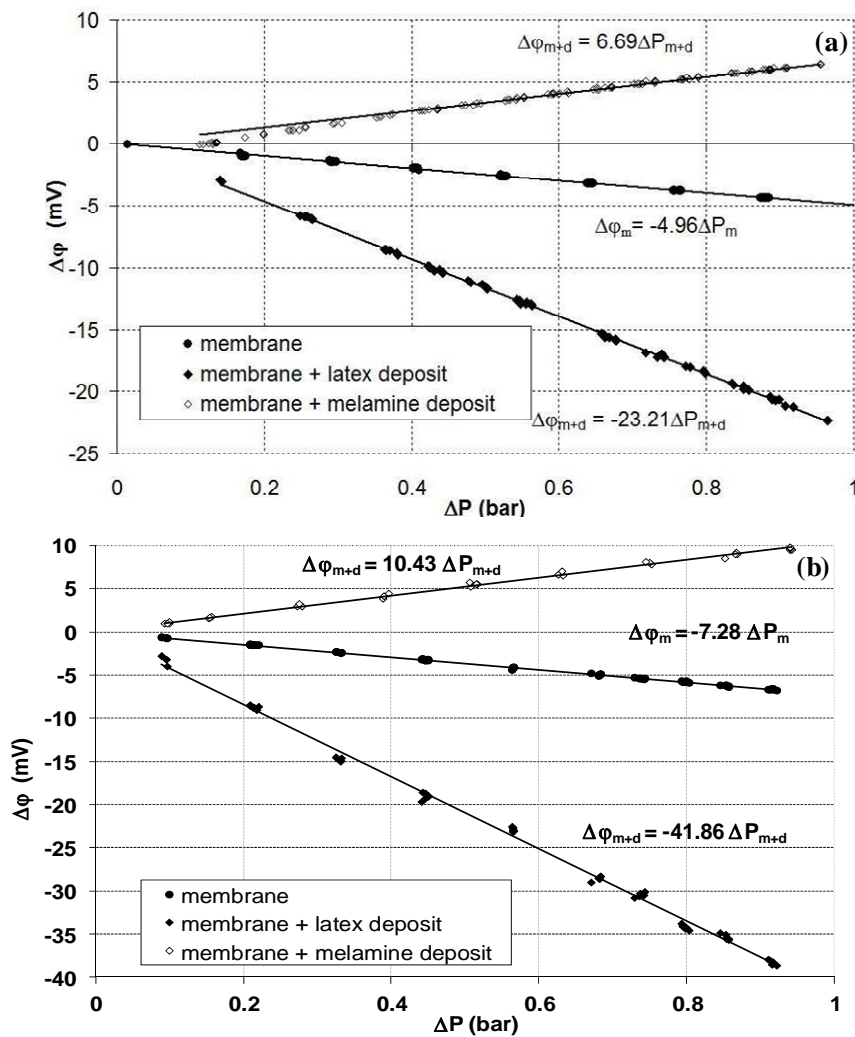


Fig. 6 Streaming potential ( $\Delta\phi$ ) vs. applied pressure difference ( $\Delta P$ ) in  $10^{-3}$  M KCl in the case of (a) flat membranes and (b) hollow fibers. The streaming potential of the membrane was measured using the method by pressure steps (pressure steps from 0 to 1 bar). The streaming potential of the “membrane + deposit” structure (deposited mass of 55 and 110  $\text{g m}^{-2}$  for flat and hollow fiber membranes, respectively) was measured at the end of stage 3 for various decreasing pressure values from  $\sim 1$  to 0 bar

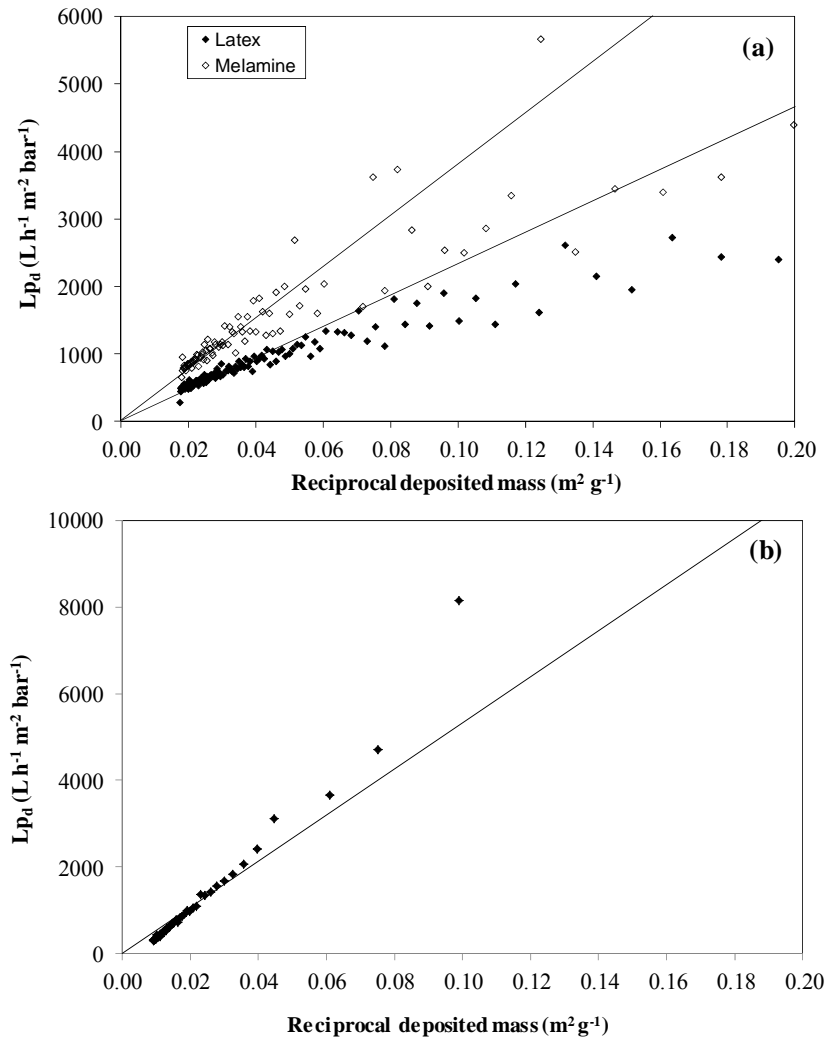


Fig. 7 Deposit permeability ( $Lp_d$ ) vs. reciprocal deposited particle mass during filtration of (a) latex and melamine suspensions at 450 mg L<sup>-1</sup> through flat membranes and (b) a latex suspension at 750 mg L<sup>-1</sup> through the hollow fiber. The straight lines show the linear dependence of  $Lp_d$  on  $A_m/m_d$  at high deposited mass ( $m_d/A_m > \sim 25$  g m<sup>-2</sup>, i.e.,  $A_m/m_d < \sim 0.04$  m<sup>2</sup> g<sup>-1</sup>). According to Eqs. (5) and (6), this behavior means that the overall porosity of deposits does not vary significantly with mass of deposited particles at high deposited mass

deposits and +8.4 mV for melamine deposits, using the well-known Helmholtz–Smoluchowski relation (Hunter 1981). Nevertheless, these values are rough because the Helmholtz–Smoluchowski relation may not be strictly valid in the experimental conditions of the study. Indeed, the thickness of the electric double layer ( $\sim 10$  nm) is comparable to the pore radius of cakes. From a theoretical calculation, in the case of the hexagonal compact packing, the pore radius in the cake layer is expected to be equal to around 40 nm (Jons *et al.* 1999). In these

conditions, the pore conductivity might be higher than the bulk conductivity. The use of the Helmholtz–Smoluchowski relation would then lead to underestimation of the true zeta potential.

In order to validate the streaming potential method at constant pressure in another way, the streaming potential coefficient of the fouled membranes was also assessed from measurements performed at various pressures by releasing pressure, at the end of the stage 3, from  $\sim 1$  to 0 bar (decreasing pressure steps were then applied). Figs. 6(a) and (b) presents typical examples of such measurements for flat and hollow fiber membranes, respectively. Streaming potentials of clean membranes (before fouling), which were measured using the method by pressure steps (increasing pressure steps in the 0-1 bar range were applied), are also shown. As can be seen, the streaming potential of fouled membranes varies linearly with pressure on the studied pressure range, which means that the overall streaming potential coefficient  $SP_{m+d}$  is independent on pressure up to 1 bar.

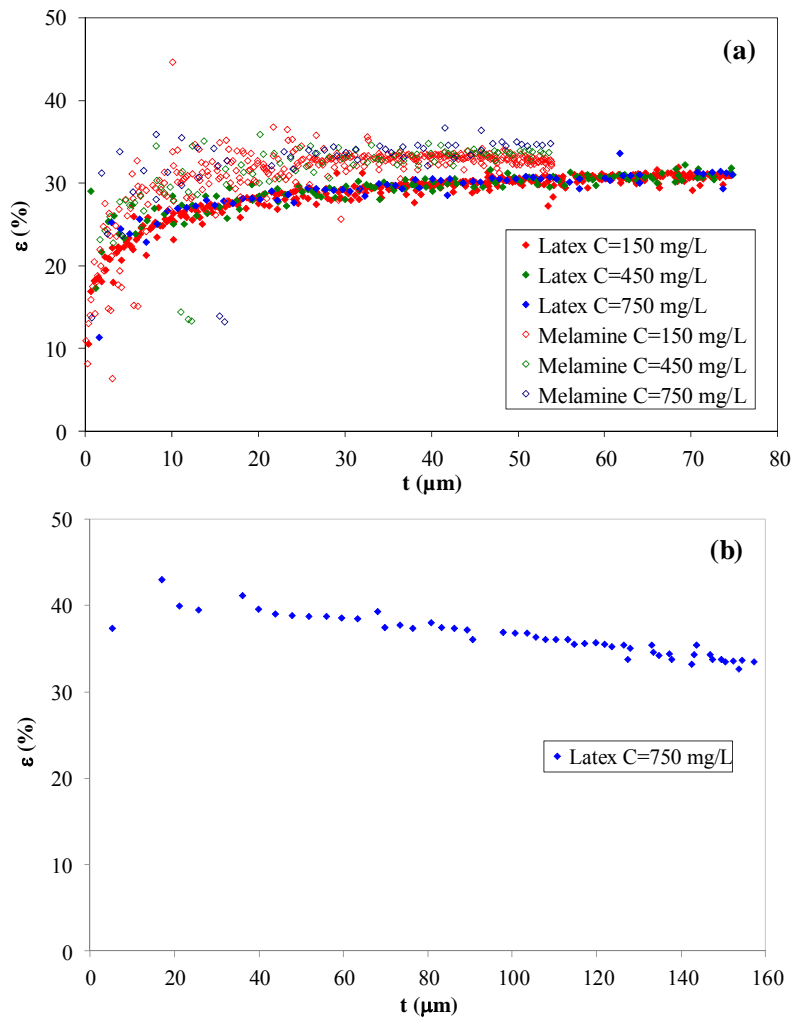


Fig. 8 Porosity ( $\epsilon$ ) vs. thickness ( $t$ ) for latex and melamine deposits build up on the (a) flat membranes and (b) hollow fiber. Latex and melamine suspensions at 150, 450 and 750  $\text{mg L}^{-1}$

This pressure independence of  $SP_{m+d}$  justifies the use of Eq. (1). It is also seen that streaming potential coefficients of fouled membranes calculated from the slopes of regressed lines are close to those obtained by the method at constant pressure, which confirms the reliability of the constant-pressure method.

The variation of  $\varepsilon$  versus deposit thickness for latex and melamine deposits build up on the flat membranes is shown in Fig. 8(a). It should be noted that  $\varepsilon$  data for thicknesses less than  $5\ \mu\text{m}$ , which represents 8-10 layers of particles, are not really reliable due to the too small contribution of deposit to the overall resistance. Moreover, all porosity value less than 26% cannot be considered as reliable since this value corresponds to the minimum porosity that can be obtained for a deposit build up from mono-dispersed rigid spherical particles. As can be seen, the porosity of the deposits levels off rather quickly, i.e., for deposit thickness greater than  $15\text{-}20\ \mu\text{m}$  and does not appear to be significantly affected by the particle concentration for the studied concentrations. Chun *et al.* (2004) showed that the increase in latex concentration led to an increase in the packing density in the cake layer (i.e., a decrease in the cake porosity). According to their relation giving the cake porosity as a function of latex concentration, a porosity variation of less than 3% should have been observed between  $150$  and  $750\ \text{mg L}^{-1}$ . Therefore these concentrations are then too close to observe a significant variation of the porosity. Porosities of 31 and 33% are obtained for latex and melamine deposits, respectively. These values indicate that deposits have a compact structure close to a hexagonal packing (Jons *et al.* 1999) as could be expected in the case of mono-dispersed rigid spherical particles. Porosity around 40% for deposit thicknesses greater than  $40\ \mu\text{m}$  was reported by Mendret *et al.* (2009) in the case of bentonite deposits. This higher porosity as compared with the ones found in the present work is probably due to the parallelepiped shape of bentonite particles. Indeed, simulation results showed that the particle shape played the major role in the porosity of the cake formed by uniform-sized spheroidal particles during the cake filtration, the structure of the cake becoming looser as the shape of the particles departed from spherical (Hwang *et al.* 1996). It should be noted that the no-variation of  $\varepsilon$  with thickness shows that physico-chemical interactions, such as electrostatic forces between particles, are negligible compared to the hydrodynamic force. Fig. 8(b) displays the variation of  $\varepsilon$  versus the thickness of a latex deposit build up on the hollow fiber surface from a particle suspension at  $750\ \text{mg L}^{-1}$  in  $10^{-3}\ \text{M KCl}$ . As explained previously, measurements can be considered as reliable when the contribution of deposit to the overall resistance becomes sufficient. By considering the same permeability drop (i.e.,  $\sim 15\%$ ) as that determined with flat membranes, a deposit thickness of  $\sim 20\ \mu\text{m}$  is estimated. It would be expected that this value is lower as that for flat membranes ( $\sim 20\ \mu\text{m}$ ) due to higher permeability of hollow fibers. Actually, this result is explained by the larger initial porosity of the cake. Unlike deposits build up on the flat membranes, a slightly decreasing trend of  $\varepsilon$  with increasing thickness is observed in Fig. 8(b). However, a similar porosity value ( $\sim 33\%$ ) is obtained for large deposit thicknesses ( $145\text{-}160\ \mu\text{m}$ ).

## 5. Conclusions

The method developed to determine the streaming potential coefficient of particle deposits ( $SP_d$ ) during dead-end filtration was validated by the independence of the streaming potential coefficient of deposits with respect to deposit thickness and growth kinetics. It was observed that  $SP_d$  levelled off much more quickly when suspensions were filtrated through the flat membranes in comparison with hollow fibers. This result could be due to a non-uniform distribution of the

deposit thickness along the membrane given that the measuring electrodes are not positioned at the same place for the two cells. The axial-position dependence of the streaming potential coefficient could then provide useful information on the deposit non-uniformity along the channel.

The method at constant pressure has the great advantage of not changing the deposit structure, whereas the “pressure steps” standard method may affect the density of the cakes, which are known to be compressible. A densification of the deposit structure with applied pressure would lead to the variation of the measured streaming potential coefficients with pressure. This new method should help to better understand the cake formation in conjunction with operating conditions in confined geometry.

## References

- Chun, M.S. and Park, W.C. (2004), “Time evolution of electrokinetic flow-induced streaming potential and flux in dead-end and cross-flow filtration of colloids through nanopores”, *J. Membr. Sci.*, **243**(1-2), 417-424.
- Chun, M.S., Cho, H.I. and Song, I.K. (2002), “Electrokinetic behavior of membrane zeta potential during the filtration of colloidal suspensions”, *Desalination*, **148**(1-3), 363-368.
- Chloe, T.B., Masse, P., Verdier, A. and Clifton, M.J. (1986), “Flux decline in batch ultrafiltration: Concentration, polarization and cake formation”, *J. Membr. Sci.*, **26**(1), 1-15.
- Gourgues, C., Aimar, P. and Sanchez, V. (1992), “Ultrafiltration of bentonite suspensions with hollow fiber membranes”, *J. Membr. Sci.*, **74**(1-2), 51-69.
- Hamachi, M. and Mietton-Peuchot, M. (1999), “Experimental investigation of cake characteristics in crossflow microfiltration”, *Chem. Eng. Sci.*, **54**(18), 4023-4030.
- Hunter, R.J. (1981), *Zeta potential in Colloid Science, Principles and Applications*, Academic Press, San Diego, CA, USA.
- Hwang, K.J., Wu, Y.S. and Lu, W.M. (1996), “The surface structure of cake formed by uniform sized rigid spheroids in cake filtration”, *Powder Tech.*, **87**(2), 161-168.
- Jons, S., Ries, P. and McDonald, C.J. (1999), “Porous latex composite membranes: Fabrication and properties”, *J. Membr. Sci.*, **155**(1), 79-99.
- Karode, S.K. (2001), “Unsteady state flux response: A method to determine the nature of the solute and gel layer in membrane filtration”, *J. Membr. Sci.*, **188**(1), 9-20.
- Le Bolay, N. and Ricard, A. (1995), “Streaming potential in membrane processes: microfiltration of egg proteins”, *J. Colloid Interface Sci.*, **170**(1), 154-160.
- Mendret, J., Guigui, C., Cabassud, C. and Schmitz, P. (2010), “Numerical investigations of the effect of non-uniform membrane permeability on deposit formation and filtration process”, *Desalination*, **263**(1-3), 122-132.
- Mendret, J., Guigui, C., Schmitz, P. and Cabassud, C. (2009), “In situ dynamic characterisation of fouling under different pressure conditions during dead-end filtration: Compressibility properties of particle cakes”, *J. Membr. Sci.*, **333**(1-2), 20-29.
- Murase, T., Ohn, T. and Kimata, K. (1995), “Filtration flux in cross flow microfiltration of dilute suspension forming a highly compressible fouling cake-layer”, *J. Membr. Sci.*, **108**(1-2), 121-128.
- Nyström, M., Kaipia, L. and Luque, S. (1995), “Fouling and retention of nanofiltration membranes”, *J. Membr. Sci.*, **98**(3), 249-262.
- Nyström, M., Pihlajamäki, A. and Ehsani, N. (1994), “Characterization of ultrafiltration membranes by simultaneous streaming potential and flux measurements”, *J. Membr. Sci.*, **87**(3), 245-256.
- Park, P.K., Lee, C.H. and Lee, S. (2007), “Determination of cake porosity using image analysis in a coagulation–microfiltration system”, *J. Membr. Sci.*, **293**(1-2), 66-72.
- Sung, J.H., Chun, M.S. and Choi, H.J. (2003), “On the behavior of electrokinetic streaming potential during protein filtration with fully and partially retentive nanopores”, *J. Colloid Interf. Sci.*, **264**(1), 195-202.

- Szymczyk, A., Fievet, P., Reggiani, J.C. and Pagetti, J. (1998), "Determination of the filtering layer electrokinetic properties of a multi-layer ceramic membrane", *Desalination*, **116**(1), 81-88.
- Szymczyk, A., Fievet, P. and Foissy, A. (2002), "Electrokinetic characterization of porous plugs from streaming potential coupled with electrical resistance measurements", *J. Colloid Interf. Sci.*, **255**(2), 323-331.
- Teychene, B., Loulergue, P., Guigui, C. and Cabassud, C. (2011), "Development and use of a novel method for *in line* characterisation of fouling layers electrokinetic properties and for fouling monitoring", *J. Membr. Sci.*, **370**(1-2), 45-47.

CC